Assessment of the Accuracy of Density Functionals for Prediction of Relative Energies and Geometries of Low-Lying Isomers of Water Hexamers

Erin E. Dahlke, Ryan M. Olson, Hannah R. Leverentz, and Donald G. Truhlar*

Department of Chemistry and Supercomputing Institute, University of Minnesota, Minneapolis, Minnesota 55455-0431

Water hexamers provide a critical testing ground for validating potential energy surface predictions because they contain structural motifs not present in smaller clusters. We tested the ability of 11 density functionals (four of which are local and seven of which are nonlocal) to accurately predict the relative energies of a series of low-lying water hexamers, relative to the CCSD(T)/aug′-cc-pVTZ level of theory, where CCSD(T) denotes coupled cluster theory with an interative treatment of single and double excitations and a quasi-perturbative treatment of connected triple excitations. Five of the density functionals were tested with two different basis sets, making a total of 16 levels of density functional theory (DFT) tested. When single-point energy calculations are carried out on geometries obtained with second-order Møller–Plesset perturbation theory (MP2), only three density functionals, M06-L, M05-2X, and M06-2X, are able to correctly predict the relative energy ordering of the hexamers. These three functionals predict that the range of energies spanned by the six isomers is 3.2–5.6 kcal/mol, whereas the other eight functionals predict ranges of 1.0–2.4 kcal/mol; the benchmark value for this range is 3.1 kcal/mol. When the hexamers are optimized at each level of theory, all methods are able to reproduce the MP2 geometries well for all isomers except the boat and bag isomers, and DFT optimization changes the energy ordering for seven of the 16 methods tested. The addition of zero-point energy changes the energy ordering for all of the density functionals studied except for M05-2X and M06-2X. The variation in relative energies predicted by the different methods highlights the necessity for exercising caution in the choice of density functionals used in future studies. Of the 11 density functionals tested, the most accurate results for energies were obtained with the PWB6K, MPWB1K, and M05-2X functionals.

Introduction

The simple structure of the water molecule belies the complicated interactions that are responsible for the unique properties of bulk water and ice. These properties, which include a liquid-phase density maximum, a negative volume of melting, a high heat capacity, and an uncommonly large number (13) of crystalline polymorphs,[1] are of great interest to the chemical community. As a result, there has been a great deal of work devoted to better understanding liquid water and ice, and much experimental and theoretical work has been carried out on small water clusters in the hope that these systems can serve as understandable microcosms that give insight into the more complicated bulk systems.

On the basis of the experimental and theoretical studies that have been carried out on such clusters, is it known that water clusters containing three to five water molecules are cyclic in nature (making them nearly planar), whereas larger clusters adopt more three-dimensional shapes.[2–6] The water hexamer is particularly interesting because it has many low-lying structural isomers, including quasi-planar and three-dimensional structures, that lie within only a few kilocalories per mole of each other.[2–9] To further complicate matters, it has been suggested that when one includes zero-point energy, the relative energy ordering of the hexamers is different from the order inferred from equilibrium binding energies,[10,11] making it difficult to predict the true preferred structure and making the hexamers an interesting system for evaluating different theoretical methods. In addition,

since some phases of ice, such as ice Ih, are built on structural motifs utilizing cyclic water hexamers,[1] there is interest in understanding the properties of the water hexamer to better understand the relative stabilities of the water polymorphs.

Many efforts in the literature have focused on trying to correctly predict the global minimum energy structure of the water hexamer using ab initio methods.[2–4,6–8,11,12] These studies, which have utilized both wave function theory (WFT, i.e., second-order Møller–Plesset perturbation theory, MP2[13]) and density functional theory (DFT),[14,15] have yielded a large amount of information about the structures of the various water hexamers and also their many-body effects and relative energies. In general, these studies focused on a small number of structural motifs, most commonly called the prism, cage, book, ring (or chair), boat, and bag isomers, which are so named for the structures suggested by the position of the oxygen atoms. For example, the boat structure is so named because it resembles the boat conformer of the cyclohexane molecule. However, for each placement of the oxygen atoms, there are numerous arrangements of the hydrogen atoms, and efforts have been made to enumerate all possible hydrogen-bond arrangements.[16] It has been found that for the cage structure alone, there are 27 chemically distinct hydrogen-bonded conformers, all of which fall within 10 kcal/mol of each other when optimized with the PM3[17,18] level of theory.[16] To truly determine the preferred structure of the water hexamer or to make a list of all structures that would contribute significantly to a calculation of its free

Energies and Geometries of Isomers of H₂O Hexamers

J. Phys. Chem. A, Vol. 112, No. 17, 2008 **3977**

TABLE 1: Relative Zero-Point Inclusive Binding Energies (kcal/mol)

	bag	boat	book	cage	prism	ring	range[a]	MUE[b]
CCSD(T)[c]	2.06	2.61	1.46	1.31	0.00	3.09	3.09	
MP2[c]	1.67	2.02	1.07	1.11	0.00	2.50	2.50	0.28
BLYP/6-31+G(d,p)	0.16	−0.82	−0.99	0.83	0.00	−1.00	1.83	1.98
B3LYP/6-31+G(d,2p)	0.33	−0.69	−0.74	0.73	0.00	−0.73	1.46	1.86
M06-L/aug-cc-pVTZ	3.53	5.14	3.07	1.51	0.00	5.61	5.61	1.32
PBE/aug-cc-pVTZ	1.49	0.01	−0.53	0.66	0.00	−0.01	2.02	1.54
PBE1W/6-311+G(2d,2p)	0.62	0.70	−0.08	0.92	0.00	0.69	0.99	1.09
BLYP/MG3S	0.10	−0.54	−0.76	0.70	0.00	−0.56	1.47	1.74
B3LYP/MG3S	0.71	0.11	−0.19	0.96	0.00	0.31	1.14	1.38
M06-L/MG3S	3.37	5.00	2.82	1.40	0.00	5.51	5.51	1.28
MPW1K/MG3S	−0.12	−0.74	−0.99	−0.13	0.00	−1.67	1.67	2.00
PBE/MG3S	0.77	0.95	0.05	0.93	0.00	0.97	0.97	0.95
PBE1W/MG3S	0.58	0.55	−0.11	0.89	0.00	0.55	1.00	1.17
PBEh/MG3S	0.04	−0.07	−0.74	−0.03	0.00	−0.97	1.01	1.63
MPWB1K/MG3S	2.34	1.77	1.30	1.93	0.00	2.42	2.42	0.74
M05-2X/MG3S	1.85	3.23	1.63	0.60	0.00	2.47	3.23	0.62
M06-2X/MG3S	2.31	4.12	2.11	0.55	0.00	3.48	4.12	0.93
PWB6K/MG3S	2.73	2.35	1.62	2.06	0.00	3.11	3.11	0.53

[a] Range of energies in the six isomers (i.e., highest energy to lowest energy). [b] Mean unsigned error in relative energy of 15 possible pairs of the six isomers. [c] Includes scaled MP2 zero-point energy; all other rows include scaled DFT zero-point energy.

energy of formation, one would have to perform a similar enumeration for each possible arrangement of oxygen atoms and then evaluate the energy of each at a high level of theory. One also may need to include zero-point energy and thermal effects, making this a very expensive and complicated process. Therefore, it is worthwhile to find a less expensive method, such as DFT, that can accurately reproduce results from accurate wave function-based methods.

In this study, we made no attempt to predict the global minimum structure of the water hexamer but instead were interested in determining how well DFT can perform in predicting the relative energies for a series of local minimum structures that represent different oxygen atom geometries. In particular, we were interested in assessing those kinds of density functionals that are commonly used in the simulation of liquid water and ice.

Molecular dynamics (MD) and Monte Carlo simulations that utilize DFT for calculations on water and ice have become increasingly popular in the literature. Because of the practical necessity of employing periodic boundary conditions for realistic simulations of bulk systems, these calculations are conveniently carried out using a plane wave basis set, and, as a result, many of the programs employed are limited to using density functionals that depend on only the local spin densities (local spin density approximation or LSDA) or the local spin densities and the magnitude of their gradients (the latter functionals are called generalized gradient approximations or GGAs). Recent functionals also depend on the kinetic energy densities and/or on Hartree−Fock exchange. These methods are referred to as meta GGA functionals if they include the kinetic energy densities, hybrid functionals if they include Hartree−Fock exchange, and hybrid meta functionals if they include both. Functionals without Hartree−Fock exchange are called local.

The most commonly used functionals in simulations of liquid water and ice are the local BLYP[19,20] and PBE[21] functionals, whereas for water clusters, hybrid B3LYP[19,20,22] is also popular. The B3LYP functional has recently been employed for a similar study of water[23] and methanol clusters[24] and also for simulation of liquid water.[25] Simulations that utilize the BLYP functional on liquid water have shown that the functional predicts a liquid phase that is too structured[26] and a critical temperature of 550 K that is 15% below the experimental value.[27] Because of these failings, we have previously assessed[28] the performance of

various density functionals for small water clusters in the hope of being able to ascertain their reliability for simulations and to better understand the shortcomings of each DFT method since any functional that worked well for bulk water and not for small clusters would be a fortuitous result.

An understanding of small water clusters is of importance because "investigations on small water clusters are a perfect means with which to characterize structural changes and bonding mechanisms in passing from isolated molecules to bulk states".[1] Therefore, if we are interested in determining whether a particular DFT method fails for simulations of water and ice, it is important to study the performance of these methods on small water clusters, which are far easier to understand than the bulk systems. Additionally, since the water hexamer has a number of low-lying geometric isomers and appears to be the crossover point between quasi-planar and more three-dimensional structures, the water hexamer provides a unique opportunity to examine not only energetics (which have been the focus of our previous work) but also structural data that may lend insight into the structural inconsistencies between the radial distribution functions obtained from DFT simulations of liquid water and those determined experimentally.

In our past work assessing DFT for small water clusters, we developed a new density functional, PBE1W,[28] which is a local variant of the local PBE functional; PBE1W has one parameter that is parametrized specifically for water. In addition to testing the previously mentioned functionals commonly used in the simulations of water and ice (BLYP, PBE, and B3LYP), we also tested PBE1W and seven other density functionals. These include the hybrid PBEh[29] functional, three recent functionals, namely, meta M06-L,[30] hybrid meta M05-2X,[31] and hybrid meta M06-2X,[32] which all have been shown to have excellent performance for noncovalent interactions in general,[30−33] although they need not be the best for water clusters, and the hybrid meta MPWB1K[34−36] and PWB6K[37] functionals, which are two general functionals for applications involving nonmetallic systems. MPW1K,[38] a hybrid functional that performs well for kinetics and reasonably well for noncovalent interactions,[36] also has been tested in this study. PBEh, a modification of PBE that includes 25% Hartree−Fock exchange[29] (making it a hybrid functional) was chosen because it too has been applied to water and ice simulations.[25] M06-L was included because it is a newly developed meta GGA functional that has been designed to give
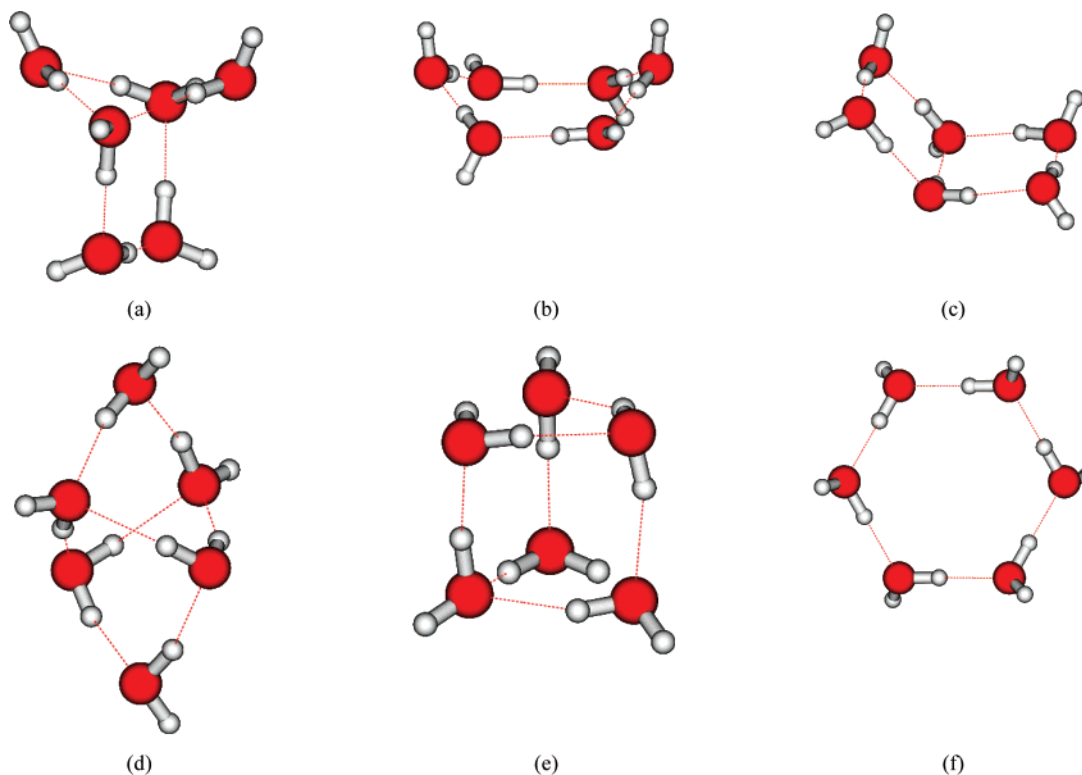
Figure 1. MP2/aug′-cc-pVTZ-optimized hexamers for the (a) bag, (b) boat, (c) book, (d) cage, (e) prism, and (f) ring structures.

an improved performance for a combination of thermochemistry, thermochemical kinetics, and organometallic, inorganometallic, biological, and noncovalent interactions, and it has a broad accuracy as compared to other local functionals. MPWB1K, MPW1K, PWB6K, M05-2X, and M06-2X were chosen because they are good general purpose functionals for applications involving thermochemistry, kinetics, and noncovalent interactions involving nonmetallic elements. Additionally, their use, along with the M06-L functional, will allow for a comparison between those functionals currently being used in simulations of water and ice and several newer functionals.

Before we begin assessing the accuracy of the DFT methods, we will examine how accurate MP2 is for these clusters since, as mentioned in the Introduction, MP2 is known to perform well for small water oligimers, but tests for larger oligomers have only recently become possible. MP2 can itself be tested by employing the more accurate coupled cluster theory with single and double excitations[39,40] and quasi-perturbative connected triple excitations[41] (CCSD(T)). Olson et al.[42] examined the binding energies of five water hexamers at the MP2 and CCSD(T) levels of theory with the aug′-cc-pVTZ basis set. They found that CCSD(T) predicted the relative energy spacings to be slightly larger than MP2 but that both methods predicted the same energy ordering. We note that MP2 is commonly used[6,43-45] for benchmark energies of water oligimers when CCSD(T) is too expensive, but in the present case, we used new state-of-the-art capabilities[42] to calculate benchmark results at the higher CCSD(T) level.

Computational Methods

Six low-lying water hexamers were chosen for this study, and we will refer to them as the bag, boat, book, cage, prism, and ring structures (see Figure 1). PM3-optimized structures for the cage, book, and prism were taken from the work of Tissandier et al.[16] with no modification and were optimized at the MP2/aug′-cc-pVTZ level of theory, where aug′-cc-pVTZ

denotes the aug-cc-pVTZ[46] basis set on oxygen and the cc-pVTZ[47,48] basis set on hydrogen. Structures for the bag, boat, and ring were based on structures shown in Figure 1 of Losada and Leutwyler[11] (the structures are denoted bag, boat, and chair, respectively, in that work) and optimized also at the MP2/aug′-cc-pVTZ level of theory. All structures were verified to be local minima by harmonic frequency analysis. Single-point CCSD-(T)/aug′-cc-pVTZ calculations were carried out on the MP2/aug′cc-pVTZ geometries to provide accurate energies for these clusters; however, because MP2 is known[42,49-51] to be very accurate for small water oligomers, we also report the MP2 results. The MP2 optimizations were carried out using Gaussian 03;[52] the MP2 frequency and CCSD(T) energy calculations were carried out using the GAMESS[42,53-55] software package (version 24 MAR 2007 (R2)). Single-point energy calculations and gas-phase optimizations were carried out on the MP2-optimized geometries with 11 density functionals: BLYP, B3LYP, MPWB1K, MPW1K, M05-2X, M06-2X, M06-L, PBE, PBEh, PBE1W, and PWB6K. All resulting structures were verified to be local minima through harmonic frequency analysis.

The BLYP, B3LYP, MPW1K, PBE, PBEh, and PBE1W calculations were carried out with the Gaussian 03 electronic structure package. The MPWB1K, M05-2X, M06-2X, M06-L, and PWB6K calculations were carried out with a locally modified version (MN-GFM[56]) of Gaussian 03.

As in previous work, all functionals were tested with the MG3S[57] basis set (which for water is the same as the 6-311+G-(2df,2p)[58] basis set), and five of the functionals (BLYP, B3LYP, PBE, PBE1W, and M06-L) were also tested with the empirically optimal basis set, specific to each functional, as determined using a method described previously.[59] The basis sets that were considered in making this determination are as follows: 6-31+G-(d,p),[60] 6-31+G(d,2p),[60] 6-311+G(2d,2p),[58] 6-311+G(2df, 2p),[58] aug-cc-pVDZ,[46] and aug-cc-pVTZ.[46,48] The optimal basis sets for the various density functionals were determined to be BLYP/

Energies and Geometries of Isomers of H$_2$O Hexamers

J. Phys. Chem. A, Vol. 112, No. 17, 2008 **3979**

TABLE 2: Relative Binding Energies (kcal/mol) for Optimized Geometries

	bag	boat	book	cage	prism	ring	MUE[a]
best estimate[b]	1.57	2.84	0.71	0.21	0.00	1.83	
MP2/aug′-cc-pVTZ	1.18	2.25	0.31	0.01	0.00	1.25	0.28
BLYP/6-31+G(d,p)	−0.38	−0.74	−1.78	−0.25	0.00	−2.19	2.00
B3LYP/6-31+G(d,2p)	−0.11	−0.48	−1.41	−0.20	0.00	−1.77	1.82
M06-L/aug-cc-pVTZ	2.72	5.14	2.38	0.46	0.00	4.26	1.25
PBE/aug-cc-pVTZ	1.02	0.03	−1.28	−0.39	0.00	−1.02	1.51
PBE1W/6-311+G(2d,2p)	0.16	0.76	−0.80	−0.08	0.00	−0.29	1.06
BLYP/MG3S	−0.35	−0.50	−1.49	−0.29	0.00	−1.59	1.73
B3LYP/MG3S	0.24	0.26	−0.91	−0.08	0.00	−0.87	1.39
M06-L/MG3S	2.91	5.06	2.42	0.52	0.00	4.07	1.14
MPW1K/MG3S	0.59	0.60	−0.54	0.05	0.00	−0.54	1.24
PBE/MG3S	0.32	0.99	−0.67	−0.05	0.00	−0.09	0.96
PBE1W/MG3S	0.14	0.63	−0.83	−0.07	0.00	−0.44	1.15
PBEh/MG3S	0.73	1.23	−0.32	0.11	0.00	0.08	0.90
MPWB1K/MG3S	1.70	2.04	0.66	0.29	0.00	0.95	0.56
M05-2X/MG3S	2.97	4.70	2.17	0.81	0.00	3.59	0.85
M06-2X/MG3S	3.01	5.68	2.99	0.94	0.00	4.61	1.40
PWB6K/MG3S	1.96	2.68	1.00	0.41	0.00	1.60	0.32

[a] MUE denotes mean unsigned error; see Results and Discussion for an explanation. [b] CCSD(T)/aug′-cc-pVTZ//MP2/aug′-cc-pVTZ.

6-31+G(d,p), B3LYP/6-31+G(d,2p), M06-L/aug-cc-pVTZ, PBE/aug-cc-pVTZ, and PBE1W/ 6-311+G(2d,2p).

Another issue worth discussing is basis set superposition error, in particular, whether counterpoise corrections[61] should be considered. In this work, we considered only relative energies between the clusters, making the definition of how one would carry out a counterpoise correction ambiguous, and therefore, no counterpoise corrections were carried out. Additionally, we were interested in validating the methods for use in condensed-phase simulations, and it is impractical to include counterpoise corrections in model chemistry for condensed-phase systems.

Results and Discussion

As mentioned in the Introduction, it has been observed that the relative ordering of the water hexamer structures can differ between the zero-point inclusive and zero-point exclusive binding energies. In the work of Losada and Leutwyler,[11] it was found that for the five isomers studied at the MP2/aug-cc-pVDZ level of theory, the energy ordering changed when the zero-point energy was included. Kozmutza et al.[10] discovered similar results for the same level of theory when they considered a series of 15 structures. Anharmonicity has only a small effect on the relative energies of the isomers;[62] therefore, we optimized each hexamer structure and determined the zero-point energy for each structure, at each level of theory, by applying an empirical scaling factor to the harmonic frequencies as determined using a method explained elsewhere.[63] (These scaling factors are given in the Supporting Information.) Table 1 shows the relative zero-point inclusive binding energies for the 16 DFT methods (where a method or level consists of a functional choice and a basis set) along with the MP2/aug′-cc-pVTZ and CCSD(T)/aug′-cc-pVTZ results (the scaled MP2/aug′-cc-PVTZ zero-point energy was added onto the CCSD(T) electronic energy for the best estimate). The range of binding energies (highest to lowest) for each method is given in the second to last column of Table 1. With six hexamer structures, one can compute 15 different energy differences between the isomers (i.e., the energy spacings between the boat and the cage or between the book and the ring structures). These 15 quantities were calculated for each of the 16 DFT methods and for the MP2/aug′-cc-pVTZ and CCSD(T)/aug′-cc-pVTZ levels of theory. The MUE for each of the DFT methods and MP2/aug′-cc-pVTZ is given in the last column of Table 1.

When the zero-point energy is included, CCSD(T) predicts the energy ordering to be prism < cage < book < bag < boat

< ring with a range of 3.09 kcal/mol. Analysis of Table 1 shows that only two methods correctly reproduce the energy ordering predicted by CCSD(T): M06-L/aug-cc-pVTZ and M06-L/ MG3S. It is interesting to note that MP2, which is usually considered to be accurate for water oligomers, and is often used in benchmark studies when CCSD(T) is not affordable, does not reproduce the energy ordering of CCSD(T) when the zero-point energy is included. MP2 overstabilizes the book isomer and predicts a relative energy ordering of prism < book < cage < bag < boat < ring. MP2 also predicts a smaller range in values (2.50 kcal/mol as compared to 3.09 kcal/mol for CCSD-(T)). However, if one looks at the mean unsigned error relative to CCSD(T) (the last column of Table 1), MP2 has the lowest error of any of the methods tested.

As mentioned previously, the only DFT methods to correctly reproduce the energy ordering predicted by CCSD(T) are M06-L/aug-cc-pVTZ and M06-L/MG3S. Of the 16 DFT methods tested, only seven correctly predict the prism to be the lowest energy isomer. Six of the DFT methods predict the book to be the lowest energy isomer (which is the third lowest energy isomer for CCSD(T)), and three methods predict the ring structure to be lowest energy isomer (which is the highest energy isomer predicted by CCSD(T)).

Examination of the range of energies predicted by each DFT methods shows that only two methods predict a range within 0.5 kcal/mol of that predicted by CCSD(T): M05-2X/MG3S and PWB6K/MG3S. Of the remaining 14 methods, 11 have ranges that are too small (by an average of 1.54 kcal/mol), and three predict ranges that are too large (by an average of 1.99 kcal/mol). Included in the three methods with ranges that are too large are M06-L/aug-cc-pVTZ and M06-L/MG3S, which are the only two to correctly predict the relative energy ordering. While both methods correctly predict the energy ordering, they predict energy spacings that are too large for all of the isomers.

Analysis of the MUE for each of the DFT methods shows that most of the methods have mean unsigned errors on the order of 1−2 kcal/mol. In particular, the GGA, meta GGA, and hybrid methods (BLYP, B3LYP, M06-L, MPW1K, PBE, and PBE1W) all have MUEs in excess of 1 kcal/mol (with the lone exception of PBE/MG3S). In contrast, all of the hybrid meta functionals have errors of less than 1 kcal/mol. The best functionals in Table 1 are PWB6K, M05-2X, MPWB1K, M06-2X, and PBE, in that order.

To assess the effect of zero-point energy on the relative stabilities predicted by the DFT methods, Table 2 compares the

TABLE 3: RMSD (Å), as Compared to MP2/aug′-cc-pVTZ-Optimized Geometries

	bag	boat	book	cage	prism	ring	ave[a]
BLYP/6-31+G(d,p)	0.06	0.20	0.04	0.06	0.04	0.03	0.07/0.07
B3LYP/6-31+G(d,2p)	0.06	0.20	0.02	0.04	0.03	0.02	0.06/0.06
M06-L/aug-cc-pVTZ	0.25	0.17	0.04	0.08	0.03	0.02	0.10/0.07
PBE/aug-cc-pVTZ	0.07	0.20	0.07	0.07	0.08	0.06	0.09/0.10
PBE1W/6-311+G(2d,2p)	0.05	0.20	0.06	0.07	0.05	0.04	0.08/0.08
BLYP/MG3S	0.07	0.19	0.04	0.06	0.05	0.03	0.07/0.08
B3LYP/MG3S	0.05	0.20	0.02	0.04	0.03	0.02	0.06/0.06
M06-L/MG3S	0.21	0.10	0.04	0.09	0.04	0.03	0.09/0.06
MPW1K/MG3S	0.05	0.24	0.02	0.03	0.02	0.03	0.06/0.07
PBE/MG3S	0.06	0.20	0.07	0.06	0.05	0.06	0.08/0.09
PBE1W/MG3S	0.05	0.19	0.05	0.06	0.05	0.03	0.07/0.08
PBEh/MG3S	0.04	0.14	0.04	0.04	0.03	0.04	0.06/0.06
MPWB1K/MG3S	0.06	0.33	0.02	0.04	0.02	0.02	0.08/0.09
M05-2X/MG3S	0.16	0.13	0.04	0.08	0.03	0.03	0.08/0.06
M06-2X/MG3S	0.47	0.39	0.04	0.12	0.05	0.04	0.18/0.14
PWB6K/MG3S	0.06	0.41	0.03	0.04	0.02	0.03	0.10/0.11
Ave	0.12(0.11)[b]	0.28	0.06	0.08	0.06	0.05	0.11/0.10

[a] Average of six previous columns followed by the average of the five previous columns. [b] Value in parentheses is the average excluding the M06-L/aug-cc-pVTZ and M06-L/MG3S data.

TABLE 4: Average O−H Bond Length (Å) for Each Isomer and for Water Monomer

	bag	boat	book	cage	prism	ring	ave	monomer[a]	MUE[b]
MP2/aug′-cc-PVTZ	0.973	0.972	0.972	0.972	0.972	0.972	0.972	0.961	
BLYP/6-31+G(d,p)	0.990	0.990	0.990	0.989	0.989	0.990	0.990	0.976	0.018
B3LYP/6-31+G(d,2p)	0.977	0.976	0.977	0.976	0.976	0.977	0.977	0.964	0.004
M06-L/aug-cc-pVTZ	0.970	0.970	0.970	0.971	0.970	0.970	0.970	0.959	0.002
PBE/aug-cc-pVTZ	0.987	0.987	0.987	0.986	0.985	0.987	0.987	0.970	0.014
PBE1W/6-311+G(2d,2p)	0.983	0.983	0.983	0.982	0.982	0.983	0.983	0.969	0.010
BLYP/MG3S	0.984	0.983	0.984	0.983	0.983	0.984	0.983	0.971	0.011
B3LYP/MG3S	0.972	0.972	0.972	0.972	0.971	0.972	0.972	0.961	0.000
M06-L/MG3S	0.969	0.968	0.969	0.969	0.969	0.969	0.969	0.958	0.003
MPW1K/MG3S	0.961	0.960	0.961	0.960	0.960	0.961	0.961	0.950	0.012
PBE/MG3S	0.986	0.985	0.985	0.985	0.984	0.985	0.985	0.969	0.013
PBE1W/MG3S	0.983	0.982	0.983	0.982	0.981	0.982	0.982	0.969	0.010
PBEh/MG3S	0.971	0.970	0.970	0.970	0.970	0.970	0.970	0.957	0.002
MPWB1K/MG3S	0.960	0.959	0.959	0.959	0.959	0.959	0.959	0.950	0.013
M05-2X/MG3S	0.967	0.966	0.967	0.967	0.967	0.967	0.967	0.957	0.005
M06-2X/MG3S	0.969	0.968	0.969	0.969	0.969	0.968	0.969	0.958	0.004
PWB6K/MG3S	0.958	0.957	0.958	0.958	0.958	0.958	0.958	0.948	0.015

[a] Experimental value: 0.957 Å.[68] [b] Mean unsigned error over the six isomers in comparison with the average MP2/aug′-cc-PVTZ O−H bond lengths. To calculate these MUEs, we found the difference between the average O−H (or O⋯H) distance in each MP2 isomer and the corresponding DFT isomer. Then, we found the absolute values of these differences and averaged them across the six isomers for each level of theory and called these the MUE.

relative, zero-point exclusive binding energies between the optimized structures at each level of theory. When zero-point energy is not included, CCSD(T) predicts the following stability order: prism < cage < book < bag < ring < boat. The only difference between the ordering here and the ordering in Table 1 is that the ring isomer is predicted to be more stable than the boat isomer. It is interesting to note that without zero-point energy, the MP2 level of theory predicts the same energy ordering as CCSD(T).

As was the case for the zero-point inclusive results, the M06-L/aug-cc-pVTZ and M06-L/MG3S levels of theory in Table 2 also correctly reproduced the ordering predicted by CCSD(T); however, as mentioned in the discussion of Table 1, the two methods based on the M06-L functional predicted energy spacings that were almost twice as large as CCSD(T). In addition, in Table 2, we see that the M05-2X/MG3S and M06-2X/MG3S methods also are able to correctly predict the CCSD-(T) ordering, but similar to the M06-L methods, M06-2X/MG3S predicts energy spacings that are too large by a factor of 2. Of the remaining 12 DFT methods, only two correctly predict the prism isomer to be the most stable, while six predict the book to be most stable, and four predict the ring to be the most stable. In general, the mean unsigned errors predicted by the DFT

methods do not change considerably between Tables 1 and 2. For the GGA and hybrid methods, the MUE for only two methods (PBEh/MG3S and MPW1K/MG3S) change by more than 0.15 kcal/mol. In contrast, the MUEs for the hybrid meta methods change by at least 0.18 kcal/mol, with the largest change for M06-2X/MG3S (which changes by 0.47 kcal/mol).

At this point, it is interesting to examine the differences between WFT and DFT geometries. Table 3 shows the root-mean-squared displacement (RMSD) (Å) between the optimized structures for each level of DFT and the MP2/aug′-cc-pVTZ-optimized structures, obtained using the method of Kabsch[64] as implemented in VMD-1.8.5.[65] From Table 3, it is clear that the boat isomer changes the most upon optimization, with an average RMSD value of 0.28 Å for the 13 methods tested. Looking at the optimized boat structures shows that all methods except MP2 optimize to what would be the analogous twisted-boat conformer (staying with the cyclohexane analogy for naming structures). The other five structures have average RMSD values of 0.05−0.12 Å, and we see that, in general, all of the DFT methods give RMSD values of 0.09 Å or less for the remaining five isomers. The three notable exceptions to this are the bag isomer for the M06-2X/MG3S method, which has an RMSD value of 0.47 Å, the bag isomer for the M06-L/aug-
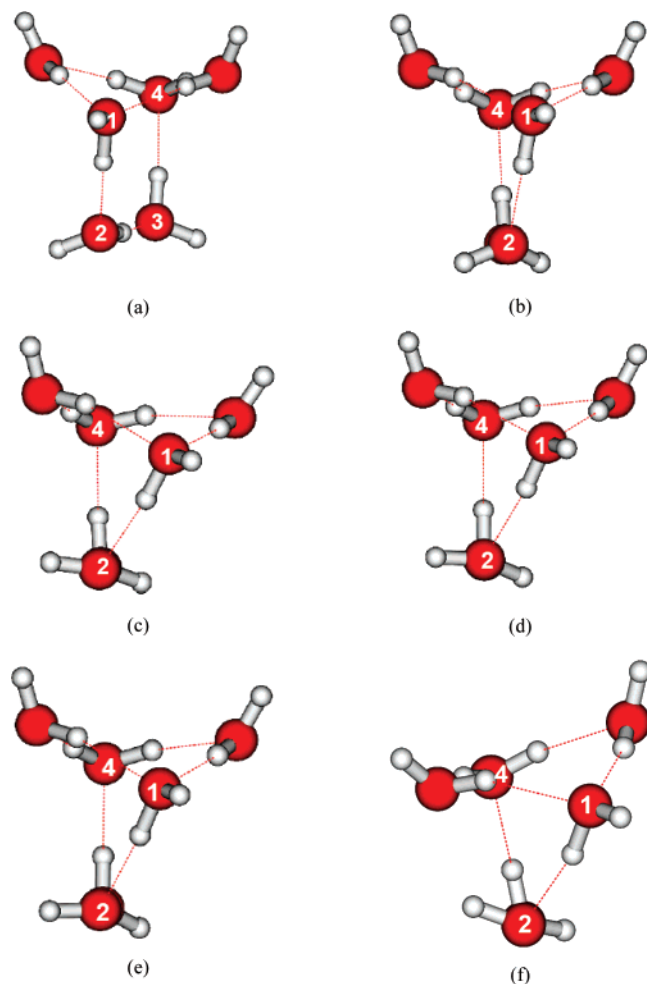
Energies and Geometries of Isomers of H$_2$O Hexamers

J. Phys. Chem. A, Vol. 112, No. 17, 2008 **3981**

Figure 2. Comparison of optimized bag isomer for selected levels of theory. (a) MP2/aug′-cc-pVTZ bag isomer from Figure 1 with oxygen atoms defining the dihedral angle ω labeled 1–4. (b) MP2/aug′-cc-pVTZ, (c) M06-L/aug-cc-pVTZ, (d) M06-L/MG3S, (e) M05-2X/MG3S, and (f) M06-2X/MG3X-optimized bag isomers are viewed down the O(2)–O(3) axis. The label for O(3) is obscured because it is directly behind O(2).

cc-pVTZ method, which has a RMSD value of 0.25 Å, and the bag isomer for the M06-L/MG3S method, which has a RMSD value of 0.21 Å. A comparison of these two structures to the MP2/aug′-cc-pVTZ structure is given in Figure 2. From Figure 2, it is clear that the largest structural difference is in the dihedral angle given by the oxygens labeled 1–4 at the top of Figure 2. In the MP2/aug′-cc-pVTZ structure, this dihedral angle, ω, has a value of $-13°$ as compared to the M06-L/aug-cc-pVTZ, M06-L/MG3S, M05-2X/MG3S, and M06-2X/MG3S structures, which have values for ω of -38, -29, -26, and $-42°$, respectively, leading to a slightly twisted structure. All other DFT methods give a value for ω that is within 6° of the MP2/aug′-cc-pVTZ value.

Table 4 lists the average covalent O–H bond length (Å) for each of the six structures and the gas-phase water molecule at the 17 levels of theory. The three GGA methods (BLYP, PBE, and PBE1W) all overestimate the average O–H bond length for all six isomers, as compared to MP2, as well as the experimental O–H bond length for the gas-phase water molecule. These results are consistent with the work of Hamprecht et al.[66] and Staroverov et al.,[67] who considered the performance of a variety of functionals for predicting the geometries of small covalently bonded molecules. M06-L,

MPWB1K, MPW1K, M05-2X, M06-2X, and PWB6K all give shorter average O–H bond lengths than MP2; however, if one compares gas-phase monomer O–H bond lengths predicted for the gas-phase water molecule, the M06-L, M05-2X, and M06-2X methods predict a more accurate bond length than MP2. Since the experimental bond lengths for the water hexamers are not known, we cannot say which methods are correct but only what the differences between the methods are. In the case of B3LYP, the O–H bond lengths predicted when the 6-31+G-(d,2p) basis set is used are systematically too long; however, when the MG3S basis set is used, the DFT and MP2 bond lengths agree to within 0.001 Å for all six structures and for the gas-phase monomer.

Table 5 lists the average hydrogen-bonded O···H distances (Å) for each hexamer and the gas-phase water dimer at each of the 17 levels of theory. Comparing the gas-phase dimer results to the best estimate shows that the MP2/aug′-cc-pVTZ result is accurate and that the M06-L/MG3S and PWB6K/MG3S results agree to within 0.001 Å. Five of the methods tested (BLYP/MG3S, B3LYP/MG3S, MPWB1K/MG3S, M05-2X/MG3S, and PWB6K/MG3S) systematically overestimate the average hydrogen-bond length for all six structures, and two of the methods (PBE/aug-cc-pVTZ and PBE/MG3S) systematically underestimate the average hydrogen-bond length in all six structures. The remaining nine methods do not appear to show any systematic trend.

The final consideration to examine is how well single-point DFT energies can reproduce wave function results for a given geometry (i.e., we do not optimize the structures with DFT). To assess this, we have carried out single-point energy calculations on the MP2/aug-cc-pVTZ geometry for each cluster with each DFT method. These results are shown in Table 6.

A comparison of the results in Table 6 to those in Table 2 shows that the energy ordering changes for half of the levels of theory (BLYP/6-31+G(d,p), B3LYP/6-31+G(d,2p), M06-L/aug-cc-pVTZ, BLYP/MG3S, PBE1W/MG3S, M06-L/MG3S, PBEh/MG3S, and MPW1K/MG3S). Significantly, however, the relative energy differences do not change much upon geometry optimization. This indicates that since many of the DFT methods predict energy spacings that are considerably smaller than those predicted by CCSD(T), a small change in these spacings is enough to change the relative ordering. If one computes the mean unsigned difference (MUD) between the relative energies of the optimized structures (Table 2) and the relative energies predicted from the single-point calculations (Table 6), the largest MUD is for PBE/aug-cc-PVTZ (0.39 kcal/mol); all other DFT methods have an MUD of 0.23 kcal/mol or less. Similarly, if we compute the MUE for each method (as described in the previous paragraph), we see that the MUEs change by at most 0.24 kcal/mol (PBE/aug-cc-pVTZ) and that on average, for the 15 other DFT methods, they change by only 0.05 kcal/mol upon optimization.

The first two rows of Table 6 compare the relative binding energies obtained in the present work at the MP2/aug′-cc-pVTZ and CCSD(T)/aug′-cc-pVTZ levels. The results here are consistent with the result of Olson et al.[42] despite the different geometries used in the two studies (Olson et al. used the MP2/DH(d,p) geometries of Day et al.[3]); the MP2 energy spacings are smaller than the CCSD(T) energy spacings by an average of 0.43 kcal/mol, but both predict the same relative energy ordering (prism < cage < book < bag < ring < boat). The former shows that MP2 is not accurate enough to serve as a benchmark for hexamers, and the latter provides some justification for using the MP2 geometries.

TABLE 5: Average Hydrogen-Bonded O···H Bond Length (Å) for Each Isomer and for Water Dimer

	bag	boat	book	cage	prism	ring	ave	dimer[a]	MUE[b]
MP2/aug′-cc-PVTZ	1.803	1.734	1.798	1.867	1.938	1.728	1.811	1.949	
BLYP/6-31+G(d,p)	1.788	1.704	1.783	1.873	1.950	1.696	1.799	1.932	0.018
B3LYP/6-31+G(d,2p)	1.800	1.715	1.792	1.877	1.952	1.708	1.808	1.932	0.012
M06-L/aug-cc-pVTZ	1.814	1.747	1.802	1.861	1.925	1.742	1.815	1.956	0.010
PBE/aug-cc-pVTZ	1.753	1.672	1.748	1.831	1.921	1.665	1.765	1.939	0.046
PBE1W/6-311+G(2d,2p)	1.803	1.720	1.796	1.881	1.956	1.713	1.811	1.923	0.010
BLYP/MG3S	1.828	1.744	1.821	1.906	1.980	1.738	1.836	1.974	0.025
B3LYP/MG3S	1.825	1.743	1.817	1.898	1.970	1.738	1.832	1.958	0.021
M06-L/MG3S	1.822	1.763	1.813	1.871	1.933	1.758	1.827	1.948	0.017
MPW1K/MG3S	1.808	1.728	1.800	1.873	1.943	1.722	1.812	1.935	0.005
PBE/MG3S	1.764	1.682	1.758	1.840	1.914	1.676	1.772	1.925	0.039
PBE1W/MG3S	1.805	1.721	1.799	1.884	1.959	1.715	1.814	1.958	0.011
PHEH/MG3S	1.789	1.709	1.783	1.860	1.931	1.702	1.796	1.931	0.015
MPWB1K/MG3S	1.839	1.764	1.831	1.897	1.962	1.757	1.842	1.963	0.031
M05-2X/MG3S	1.830	1.764	1.826	1.886	1.948	1.758	1.836	1.966	0.024
M06-2X/MG3S	1.883	1.748	1.801	1.859	1.920	1.738	1.825	1.945	0.022
PWB6K/MG3S	1.841	1.765	1.834	1.900	1.967	1.760	1.845	1.950	0.033

[a] Best estimate: 1.949 Å (from a CCSD(T)/TZ2P(f,d) + dif calculation). [b] Mean unsigned error over the six isomers in comparison with the average MP2/aug′-cc-PVTZ O···H bond lengths. See explanation in Table 4.

TABLE 6: Relative Binding Energies[a] (kcal/mol) for MP2/aug′-cc-pVTZ-Optimized Geometries

	bag	boat	book	cage	prism	ring	MUE[b]
CCSD(T)/aug′-cc-pVTZ//[c]	1.57	2.84	0.71	0.21	0.00	1.83	
MP2/aug′-cc-pVTZ	1.18	2.25	0.31	0.01	0.00	1.25	0.28
BLYP/6-31+G(d,p)//	−0.42	−0.84	−1.83	−0.25	0.00	−2.31	2.06
B3LYP/6-31+G(d,2p)//	−0.12	−0.50	−1.45	−0.19	0.00	−1.82	1.84
M06-L/aug-cc-pVTZ//	2.92	5.16	2.37	0.47	0.00	4.24	1.22
PBE/aug-cc-pVTZ//	−0.05	0.34	−1.07	−0.27	0.00	−0.77	1.28
PBE1W/6-311+G(2d,2p)//	0.24	0.91	−0.70	0.02	0.00	−0.21	1.02
BLYP/MG3S//	−0.38	−0.59	−1.56	−0.25	0.00	−1.73	1.81
B3LYP/MG3S//	0.20	0.18	−0.97	−0.08	0.00	−0.97	1.44
M06-L/MG3S//	3.09	5.08	2.41	0.52	0.00	4.08	1.13
MPW1K/MG3S//	0.56	0.54	−0.58	0.03	0.00	−0.63	1.28
PBE/MG3S//	0.49	1.29	−0.47	0.05	0.00	0.13	0.84
PBE1W/MG3S//	0.17	0.69	−0.78	−0.01	0.00	−0.43	1.14
PBEh/MG3S//	0.76	1.29	−0.28	0.12	0.00	0.13	0.87
MPWB1K/MG3S//	1.70	1.95	0.60	0.31	0.00	0.82	0.63
M05-2X/MG3S//	2.99	4.68	2.16	0.84	0.00	3.53	0.83
M06-2X/MG3S//	3.64	5.50	2.84	0.91	0.00	4.41	1.25
PWB6K/MG3S//	1.96	2.56	0.94	0.44	0.00	1.45	0.40

[a] Relative to the prism isomer. [b] Mean unsigned error; see Results and Discussion for an explanation. [c] // denotes //MP2/aug′-cc-pVTZ, where aug′-cc-pVTZ denotes the use of the aug-cc-pVTZ basis set on oxygen and the cc-pVTZ basis set on hydrogen.

Of the 16 density functional methods (where we continue to use the language such that a method or level consists of a functional choice and a basis set) tested in Table 6, only four methods, M06-L/aug-cc-pVTZ, M06-L/MG3S, M05-2X/MG3S, and M06-2X/MG3S, correctly predict the CCSD(T) energy ordering (these are the same four methods that correctly predicted the ordering in Table 2). In fact, of the 16 methods tested, three (BLYP/6-31+G(d,p), B3LYP/6-31+G(d,2p), and BLYP/MG3S) predicted the prism to be the highest energy isomer. Of the 12 methods that do not get the ordering correct, two correctly predict the prism to be the lowest in energy, five predict the book to be lowest in energy, and five predict the ring to be lowest in energy.

As we have seen in both Table 2 and Table 6, the M06-L/aug-cc-pVTZ, M06-L/MG3S, M05-2X/MG3S, and M06-2X/MG3S methods predict the correct energy ordering, but they do not predict the correct energy gaps between the structures. The largest gap in our best estimate is between the prism and the boat isomers, and it is only 2.84 kcal/mol; however, the M06-L/aug-cc-pVTZ, M06-L/MG3S, M05-2X/MG3S, and M06-2X/MG3S methods predict energy differences of 5.16, 5.08, 4.68, and 5.50 kcal/mol, respectively. Even the energy spacing between the prism and the cage isomers, which are separated by only 0.21 kcal/mol at the CCSD(T) level of theory, are

predicted to be separated by 0.47 kcal/mol at the M06-L/aug-cc-pVTZ level of theory, 0.52 kcal/mol at the M06-L/MG3S level of theory, 0.84 kcal/mol at the M05-2X/MG3S level of theory, and 0.91 kcal/mol at the M06-2X/MG3S level of theory. The only density functional methods that predict the cage and prism to be nearly isoenergetic are PBE1W/6-311+G(2d,2p), PBE/MG3S, PBE1W/MG3S, and MPW1K/MG3S, with absolute energy differences of 0.02, 0.05, 0.01, and 0.03 kcal/mol, respectively.

The mean unsigned error between the DFT results and the CCSD(T) results and between the MP2 result and the CCSD-(T) result is given in the last column of Table 6. On the basis of this analysis, we see that the hybrid meta MPWB1K/MG3S and PWB6K/MG3S levels of theory have the smallest deviation with MUEs of 0.63 and 0.40 kcal/mol, respectively. If one considers only local functionals, PBE/MG3S and PBE1W/6-311+G(2d,2p) perform best with MUEs of 0.84 and 1.02 kcal/mol. Despite the large energy gaps, relative to the prism structure, predicted by the M06-L, M05-2X, and M06-2X functionals, these methods do not have the largest or second largest MUE, which are given by the BLYP/6-31+G(d,p) (2.06 kcal/mol) and B3LYP/6-31+G(2d,2p) (1.84 kcal/mol) methods. One might conclude therefore than these gaps result more from

Energies and Geometries of Isomers of H$_2$O Hexamers

J. Phys. Chem. A, Vol. 112, No. 17, 2008 **3983**

overstabilizing the prism than from a more general tendency to overestimate the energy differences.

Conclusion

In this study, we presented new benchmark results (single-point CCSD(T)/aug′-cc-pVTZ//MP2/aug′-cc-pVTZ calculations) for the relative energies of a set of low-lying water hexamers, and we used them to evaluate the accuracy of 16 combinations of density functionals and basis sets for predicting their correct energetic ordering and geometries. We found that of the 16 methods tested, only four methods, M06-L/aug-cc-pVTZ, M06-L/MG3S, M05-2X/MG3S, and M06-2X/MG3S, were able to predict correctly the relative energy ordering. The other 12 methods tested failed to predict the correct order, and in some cases, they predicted the minimum energy structure at the CCSD(T)/aug′-cc-pVTZ level of theory to be the highest energy structure. These tests are important because hexamers show new structural motifs not present in smaller clusters, but density functionals previously have not been tested against accurate benchmark results for clusters this large.

We also showed that the relative energies change very little upon reoptimization of the geometry by DFT, and we found that, in general, the density functionals tested were able to reproduce the MP2 structures well. An exception to this was the bag for which the M06-2X/MG3S, M06-L/aug-cc-pVTZ, M06-L/MG3S, and M05-2X/MG3S geometries had RMSD values of 0.47, 0.25, 0.21, and 0.16 Å, respectively. These RMSD values were significantly larger than any those for any other method for any other structure.

Finally, we found that the inclusion of scaled zero-point energy changes the relative stability of the hexamers for all methods except for the M05-2X/MG3S and M06-2X/MG3S methods. The M06-L/aug-c-pVTZ, M06-L/MG3S, M06-2X/MG3S, and M05-2X/MG3S methods are the only methods that agree with the best estimate of the zero-point inclusive energy spacings (as obtained by adding CCSD(T)/aug′-cc-pVTZ electronic energy to scaled MP2/aug′-cc-pVTZ zero-point energy). None of the 16 DFT methods predicted the same zero-point inclusive energy spacings as the scaled MP2 level of wave function theory.

The large diversity in the results illustrates the need for great care when using density functionals to study water, not only in cluster calculations such as these but also in liquid-phase and ice simulations. This is particularly true in light of our finding that none of the methods tested, which included those that are most commonly used in liquid-phase simulations, were able to correctly predict the energy ordering for this series of hexamers. In general, we saw that those methods that contain kinetic energy density gave better results than those that did not, and we suggest that M06-L may be a promising method for use on these systems for those who are limited by practical considerations to using only local functionals. More work will need to be done to determine if the large energy differences predicted by M06-L for these hexamers are present when other water systems are studied.

Supporting Information Available: Tables of (i) Cartesian coordinates for the MP2/aug′-cc-pVTZ- and DFT-optimized structures, (ii) scaling factors used for vibrational frequencies, and (iii) absolute energies (Hartrees) for optimized structures and single-point calculations at MP2/aug′-cc-pVTZ geometry, for all levels of theory. This material is available free of charge via the Internet at http://pubs.acs.org.

References and Notes

(1) Ludwig, R. *Angew. Chem.*, *Int. Ed.* **2001**, *40*, 1808.
(2) Estrin, D. A.; Paglieri, L.; Corongiu, G.; Clementi, E. *J. Phys. Chem.* **1996**, *100*, 8701.
(3) Day, P. N.; Pachter, R.; Gordon, M. S.; Merrill, G. N. *J. Chem. Phys.* **2000**, *112*, 2063.
(4) Lee, H. M.; Suh, S. B.; Lee, J. Y.; Tarakeshwar, P.; Kim, K. S. *J. Chem. Phys.* **2000**, *112*, 9759.
(5) Upadhyay, D. M.; Shukla, M. K.; Mishra, P. C. *Int. J. Quantum Chem.* **2001**, *81*, 90.
(6) Xantheas, S. S.; Burnham, C. J.; Harrison, R. J. *J. Chem. Phys.* **2002**, *116*, 1493.
(7) Mhin, B. J.; Kim, H. S.; Kim, H. S.; Yoon, C. W.; Kim, K. S. *Chem. Phys. Lett.* **1991**, *176*, 41.
(8) Tsai, C. J.; Jordan, K. D. *Chem. Phys. Lett.* **1993**, *213*, 181.
(9) Lee, C.; Chen, H.; Fitzgerald, G. *J. Chem. Phys.* **1994**, *101*, 4472.
(10) Kozmutza, C.; Kryachko, E. S.; Tfrist, E. *THEOCHEM* **2000**, *501*, 435.
(11) Losada, M.; Leutwyler, S. *J. Chem. Phys.* **2002**, *117*, 2003.
(12) Mhin, B. J.; Kim, J.; Lee, S.; Lee, J. Y.; Kim, K. S. *J. Chem. Phys.* **1993**, *100*, 4484.
(13) Møller, C.; Plesset, M. S. *Phys. Rev.* **1934**, *46*, 618.
(14) Hohenberg, P.; Kohn, W. *Phys. Rev.* **1964**, *136*, 864.
(15) Kohn, W.; Sham, L. J. *Phys. Rev.* **1965**, *140*, 1133.
(16) Tissandier, M. D.; Singer, S. J.; Coe, J. V. *J. Phys. Chem. A* **2000**, *104*, 7523.
(17) Stewart, J. J. P. *J. Comput. Chem.* **1989**, *10*, 209.
(18) Stewart, J. J. P. *J. Comput. Chem.* **1989**, *10*, 221.
(19) Becke, A. D. *Phys. Rev. A: At., Mol., Opt. Phys.* **1988**, *38*, 3098.
(20) Lee, C.; Yang, W.; Parr, R. G. *Phys. Rev. B: Condens. Matter Mater. Phys.* **1988**, *37*, 785.
(21) Perdew, J. P.; Burke, K.; Ernzerhof, M. *Phys. Rev. Lett.* **1996**, *77*, 3865.
(22) Stephens, P. J.; Devlin, F. J.; Chabalowski, C. F.; Frisch, M. J. *J. Phys. Chem.* **1994**, *98*, 11623.
(23) Maheshwary, A.; Patel, N.; Sathyamurthy, N.; Kulkarni, A. D.; Gadre, S. R. *J. Phys. Chem. A* **2001**, *105*, 10525.
(24) Boyd, S. L.; Boyd, R. J. *J. Chem. Theory Comput.* **2007**, *3*, 54.
(25) Todorova, T.; Seitsonen, A. P.; Hutter, J.; Kuo, I. W.; Mundy, C. J. *J. Phys. Chem. B* **2006**, *110*, 3685.
(26) Kuo, I.-J. W.; Mundy, C. J.; Eggimann, B. L.; McGrath, M. J.; Siepmann, J. I.; Chen, B.; Vieceli, J.; Tobias, D. J. *J. Phys. Chem. B* **2006**, *110*, 3738.
(27) McGrath, M. J.; Siepmann, J. I.; Kuo, I.-J. W.; Mundy, C. J.; VandeVondele, J.; Hutter, J.; Mohamed, F.; Krack, M. *J. Phys. Chem. A* **2006**, *110*, 640.
(28) Dahlke, E. E.; Truhlar, D. G. *J. Phys. Chem. B* **2005**, *109*, 15677.
(29) Adamo, C.; Barone, V. *J. Chem. Phys.* **1999**, 6158.
(30) Zhao, Y.; Truhlar, D. G. *J. Chem. Phys.* **2006**, *125*, 194101.
(31) Zhao, Y.; Schultz, N. E.; Truhlar, D. G. *J. Chem. Theory Comput.* **2006**, *2*, 364.
(32) Zhao, Y.; Truhlar, D. G. *Theor. Chem. Acc.* **2008**, published online at DOI 10.1007/s00214-007-0310-X and DOI 10.1007/s00214-007-0401-8.
(33) Zhao, Y.; Truhlar, D. G. *J. Chem. Theory Comput.* **2007**, *3*, 289.
(34) Adamo, C.; Barone, V. *J. Chem. Phys.* **1998**, *108*, 664.
(35) Becke, A. D. *J. Chem. Phys.* **1996**, *104*, 1040.
(36) Zhao, Y.; Truhlar, D. G. *J. Phys. Chem. A* **2004**, *108*, 6908.
(37) Zhao, Y.; Truhlar, D. G. *J. Phys. Chem. A* **2005**, *109*, 5656.
(38) Lynch, B. J.; Fast, P. L.; Harris, M.; Truhlar, D. G. *J. Phys. Chem. A* **2000**, *104*, 4811.
(39) Cizek, J. *Adv. Chem. Phys.* **1969**, *14*, 35.
(40) Purvis, G. D.; Bartlett, R. J. *J. Chem. Phys.* **1982**, *76*, 1910.
(41) Raghavachari, K.; Trucks, G. W.; Pople, J. A.; Head Gordon, M. *Chem. Phys. Lett.* **1989**, *157*, 479.
(42) Olson, R. M.; Bentz, J. L.; Kendall, R. A.; Schmidt, M. W.; Gordon, M. S. *J. Chem. Theory Comput.* **2007**, *3*, 1312.
(43) Fanourgakis, G. S.; Aprà, E.; de Jong, W. A. *J. Chem. Phys.* **2005**, 134304.
(44) Dunn, M. E.; Evans, T. M.; Kirschner, K. N.; Shields, G. C. *J. Chem. Phys. A* **2006**, *110*, 303.
(45) Park, Y. C.; Lee, J. S. *Bull. Korean Chem. Soc.* **2007**, *28*, 386.
(46) Kendall, R. A.; Dunning, T. H., Jr.; Harrison, R. J. *J. Chem. Phys.* **1995**, *96*, 6796.
(47) Dunning, T. H. *J. Chem. Phys.* **1989**, *90*, 1007.

(48) Woon, D. E.; Dunning, T. H., Jr. *J. Chem. Phys.* **1993**, *98*, 1358.

(49) Halkier, A.; Koch, H.; Jorgensen, P.; Christiansen, O.; Nielsen, I. M. B.; Helgaker, T. *Theor. Chem. Acc.* **1997**, *97*, 150.

(50) Nielsen, I. M. B.; Seidl, E. T.; Janssen, C. L. *J. Chem. Phys.* **1999**, *110*, 9435.

(51) Xantheas, S. S.; Burnham, C. J.; Harrison, R. J. *J. Chem. Phys.* **2002**, *116*, 1493.

(52) Frisch, M. J.; Trucks, G. W.; Schlegel, H. B.; Scuseria, G. E.; Robb, M. A.; Cheeseman, J. R.; Montgomery, J. A., Jr.; Vreven, T.; Kudin, K. N.; Burant, J. C.; Millam, J. M.; Iyengar, S. S.; Tomasi, J.; Barone, V.; Mennucci, B.; Cossi, M.; Scalmani, G.; Rega, N.; Petersson, G. A.; Nakatsuji, H.; Hada, M.; Ehara, M.; Toyota, K.; Fukuda, R.; Hasegawa, J.; Ishida, M.; Nakajima, T.; Honda, Y.; Kitao, O.; Nakai, H.; Klene, M.; Li, X.; Knox, J. E.; Hratchian, H. P.; Cross, J. B.; Adamo, C.; Jaramillo, J.; Gomperts, R.; Stratmann, R. E.; Yazyev, O.; Austin, A. J.; Cammi, R.; Pomelli, C.; Ochterski, J. W.; Ayala, P. Y.; Morokuma, K.; Voth, G. A.; Salvador, P.; Dannenberg, J. J.; Zakrzewski, V. G.; Dapprich, S.; Daniels, A. D.; Strain, M. C.; Farkas, O.; Malick, D. K.; Rabuck, A. D.; Raghavachari, K.; Foresman, J. B.; Ortiz, J. V.; Cui, Q.; Baboul, A. G.; Clifford, S.; Cioslowski, J.; Stefanov, B. B.; Liu, G.; Liashenko, A.; Piskorz, P.; Komaromi, I.; Martin, R. L.; Fox, D. J.; Keith, T.; Al-Laham, M. A.; Peng, C. Y.; Nanayakkara, A.; Challacombe, M.; Gill, P. M. W.; Johnson, B.; Chen, W.; Wong, M. W.; Gonzalez, C.; Pople, J. A. *Gaussian 03*, version c.01; Gaussian, Inc.: Pittsburgh, PA, 2003.

(53) Schmidt, M. W.; Baldridge, K. K.; Boatz, J. A.; Elbert, S. T.; Gordon, M. S.; Jensen, J. H.; Koseki, S.; Matsunaga, N.; Nguyen, K. A.; Su, S.; Windus, T. L.; Dupuis, M.; Montgomery, J. A. *J. Comput. Chem.* **1993**, *14*, 1347.

(54) Fletcher, G. D.; Schmidt, M. W.; Bode, B. M.; Gordon, M. S. *Comput. Phys. Commun.* **2000**, *128*, 190.

(55) Olson, R. M.; Schmidt, M. W.; Gordon, M. S.; Rendell, A. P. *ACM/ IEEE Supercomputing Conference Volume* **2003**, *41*, DOI 10.1109/ SC.2003.10011.

(56) Zhao, Y.; Truhlar, D. G. *MN-GFM: Minnesota Gaussian Functional Module, version 2.0.1*; University of Minnesota: Minneapolis, 2006.

(57) Lynch, B. J.; Zhao, Y.; Truhlar, D. G. *J. Phys. Chem. A* **2003**, *107*, 1384.

(58) Krishnan, R.; Binkley, J. S.; Seeger, R.; Pople, J. A. *J. Chem. Phys.* **1980**, *72*, 650.

(59) Csonka, G. I.; Ruzsinszky, A.; Perdew, J. P. *J. Phys. Chem. B* **2005**, *109*, 21471.

(60) Hehre, W. J.; Radom, L.; Schleyer, P. v. R.; Pople, J. A. *Ab Initio Molecular Orbital Theory*; Wiley: New York, 1986; p 576.

(61) Boys, S. F.; Bernardi, D. *Mol. Phys.* **1970**, *19*, 553.

(62) Diri, K.; Myshakin, E. M.; Jordan, K. D. *J. Phys. Chem. A* **2005**, *109*, 4005.

(63) Fast, P. L.; Corchado, J.; Sanchez, M. L.; Truhlar, D. G. *J. Phys. Chem. A* **1999**, *103*, 3139.

(64) Kabsch, W. *Acta Crystallogr., Sect. A: Found. Crystallogr.* **1978**, *34*, 827.

(65) Humphrey, W.; Dalke, A.; Schulten, K. *J. Mol. Graphics* **1996**, *14*, 336.

(66) Hamprecht, F. A.; Cohen, A. J.; Tozer, D. J.; Handy, N. C. *J. Chem. Phys.* **1998**, *109*, 6264.

(67) Staroverov, V.; Scuseria, G. E.; Toa, J.; Perdew, J. P. *J. Chem. Phys.* **2003**, *119*, 12129.

(68) Hasted, J. B. In *Water: A Comprehensive Treatise*; Franks, F., Ed.; Plenum Press: New York, 1972; pp 255−309.